Journal of Organometallic Chemistry 694 (2009) 4241–4249

Contents lists available at ScienceDirect

Journal of Organometallic Chemistry

journal homepage: www.elsevier.com/locate/jorganchem

Reactions of $Co_2(CO)_8$ and of $Co_2(CO)_6L$ (L = 3-pentyn-1-ol, 1,4-butyn-diol or 2-methyl-3-butyn-2-ol) with 2(diphenylphosphino)ethyl-trietoxysilane and tris(hydroxymethyl)phosphine for applications to new sol–gel materials

Fabio Carniato [a], Giorgio Gatti [a], Giuliana Gervasio [b], Domenica Marabello [b,*], Enrico Sappa [a,*], Andrea Secco [a]

[a] Dipartimento di Scienze e Tecnologie Avanzate, Centro Interdisciplinare Nano-Sistemi, Università del Piemonte Orientale, Via Teresa Michel 11, I-15100 Alessandria, Italy
[b] Dipartimento di Chimica IFM, Università di Torino, Centro Interdipartimentale di Cristallografia Diffrattometrica CrisDi, via Pietro Giuria 7, I-10125 Torino, Italy

ARTICLE INFO

Article history:
Received 15 July 2009
Received in revised form 29 August 2009
Accepted 31 August 2009
Available online 4 September 2009

Keywords:
Cobalt carbonyls
Functionalized alkynes
Triethoxysilyl ligands
Sol–gel inorganic–organometallic materials
Molecular structure

ABSTRACT

The complex $Co_2(CO)_6[\mu\text{-}\eta^2\text{-}(H_3CC{\equiv}CCH_2CH_2OH)]$ (**1**) with the ligand 3-pentyn-1-ol (*pol*) has been synthesized following established procedures. Its structure has been determined by X-ray analysis. The complex $Co_2(CO)_6$(*mbo*) (*mbo* = 2-methyl-3-butyn-2-ol, $HC{\equiv}CC(CH_3)_2OH$), (**3**), along with the already known $Co_2(CO)_6$(*bud*) (*bud* = 1,4-butyn-diol, $HOCH_2C{\equiv}CCH_2OH$) (**2**), and $Co_2(CO)_8$ were reacted with 2(diphenylphosphino)ethyl-triethoxysilane $[Ph_2PCH_2CH_2Si(OCH_2CH_3)_3]$ (*dpts*) and tris(hydroxymethyl)phosphine $[P(CH_2OH)_3]$ (*thp*). With *dpts*, mono- and di-substituted complexes were obtained: these were characterized by analytical and spectroscopic techniques. The structures of $Co_2(CO)_6$(*dpts*)$_2$ (**5**) and of $Co_2(CO)_4$(*pol*)(*dpts*)$_2$ (**8**) have been determined by X-ray analysis.

Complex (**1**) was reacted with 3-(triethoxysilyl)propyl isocyanate $[(H_3CCH_2O)_3Si(CH_2)_3NCO]$ (*tsi*): the new complex $Co_2(CO)_6[H_3CC{\equiv}CCH_2CH_2OC(=O)NH(CH_2)_3Si(OCH_2CH_3)_3]$ (**9**) was obtained and spectroscopically characterized. The complex has also been reacted with tetraethyl orthosilicate (*teos*); a new inorganic–organometallic material was obtained. Complex (**5**) has been grafted on the mesoporous material SBA-15. The hybrid inorganic–organometallic materials obtained have been characterized by inductively coupled plasma-mass spectrometry (ICP-MS), infrared spectroscopy (FT-IR) under vacuum conditions, X-ray diffraction (XRD) and scanning electron microscopy coupled to EDS probe (SEM–EDS).

1. Introduction

Hybrid inorganic–organic sol–gel materials are currently synthesized and used for example as a new class of heterogeneous catalysts [1,2]. Some silica-based inorganic–organometallic materials are also known; for example metal carbonyl clusters substituted with alkynic ligands containing OH functionalities or $Si(OCH_2CH_3)_3$ groups can be grafted to silica-based inorganic materials [3]. These syntheses are however made difficult because of exchange reactions between the coordinated alkynols and the sol–gel materials and mostly because several alkynols undergo loss of their functionalities when reacted with iron [4] or ruthenium [5] carbonyls. We have therefore attempted the synthesis of new ligands by reacting the alkynols with triethoxysilyl-propyl-isocyanate (*tsi*) $[(H_3CCH_2O)_3Si(CH_2)_3NCO]$ [6] and other alkoxysilyl-contaning ligands [7].

These ligands also, in some instances, undergo cleavage of the (O=)C–O–NH bonds giving fragments which still coordinate to metals using C=N bonds instead of the alkyne C≡C bonds [8]. As a consequence, products different from those expected are obtained, usually in low yields [7]. More recently, however, we found that 2(diphenylphosphino)ethyl-triethoxysilane (*dpts*) reacts with $Ru_3(CO)_{12}$ forming the substituted complexes $Ru_3(CO)_{12-n}L_n$ [L = $Ph_2P(CH_2)_2Si(OCH_2CH_3)_3$; *n* = 1,2] in high yields and that these complexes can be easily grafted to the mesoporous silica materials SBA-15 and MCM-41 [9].

Here we report on the reaction of $Co_2(CO)_8$ with 3-pentyn-1-ol (*pol*) which had not been previously described: we obtained very high yields of the expected $Co_2(CO)_6[\mu\text{-}\eta^2\text{-}(H_3CC{\equiv}CCH_2CH_2OH)]$ (**1**) whose structure has been determined by X-ray analysis. Complex (**1**) was reacted with 3-(triethoxysilyl)propyl isocyanate (*tsi*) and with tetraethoxysilane (*teos*); the product of the reaction with *tsi*, $Co_2(CO)_6[H_3CC{\equiv}CCH_2CH_2OC(=O)NH(CH_2)_3Si(OCH_2CH_3)_3]$, (**9**) was characterized by analytical and spectroscopic techniques. The material obtained with *teos* was also characterized by solid-state spectroscopies.

The reactions of $Co_2(CO)_8$, $Co_2(CO)_6L$ (L = *pol*, (**1**), L = *bud* (1,4-butyn-diol, $HOCH_2C{\equiv}CCH_2OH$), (**2**), L = *mbo* (2-methyl-3-butyn-2-ol, $HC{\equiv}CC(CH_3)_2OH$), (**3**)) with 2(diphenylphosphino)ethyl-triethoysilane $[Ph_2PCH_2CH_2Si(OCH_2CH_3)_3]$ (*dpts*) and tris(hydroxymethyl)phosphine $[P(CH_2OH)_3]$ (*thp*) were also

* Corresponding author.
E-mail address: sappa@unipmn.it (E. Sappa).

0022-328X/$ - see front matter © 2009 Elsevier B.V. All rights reserved.
doi:10.1016/j.jorganchem.2009.08.040

examined. These ligands could ensure a stable grafting to silica-based materials. With *dpts* mono- and di-substituted phosphinic derivatives were obtained and were characterized by analytical and spectroscopic techniques. In contrast *thp* did not give CO substitution. The structures of the complexes $Co_2(CO)_6[Ph_2PCH_2CH_2Si(OCH_2CH_3)_3]_2$ (**5**) and of $Co_2(CO)_4[\mu\text{-}\eta^2\text{-}(C{\equiv}C(CH_2OH)_2)][Ph_2PCH_2CH_2Si(OCH_2CH_3)_3]_2$ (**8**) have been determined by X-ray analyses. (**5**) has been grafted on the mesoporous SBA-15 [10] and the material obtained has been characterized by inductively coupled plasma-mass spectrometry (ICP-MS), infared spectroscopy under vacuum conditions, X-ray diffraction (XRD), and scanning electron microscopy coupled to EDS probe (SEM–EDS).

2. Experimental

2.1. General experimental details. Analysis of the products

2.1.1. Materials

$Co_2(CO)_8$ (Strem Chemicals), 3-pentyn-1-ol, 1,4-butyn-diol and 2-methyl-3-butyn-2-ol (Lancaster Syntheses) were commercial products; *tsi* and *teos* were obtained from Sigma–Aldrich. The phosphinic ligand *dpts* was from ABCR (Gelest, Karsruhe). All were used as received. Solvents (e.g. hexane, heptane, diethyl ether and toluene) were laboratory grade and were dehydrated over sodium. Ethanol, HCl (37%) and NaF were laboratory grade reagents (Carlo Erba). The reactions of (**1**) with *tsi* were performed following an already established procedure [6]. The reactions of (**1**) with *teos* and those of (**5**) with SBA-15 are described below.

2.1.2. Synthesis of (*1*) and of the phosphine-substituted dicobalt complexes

All the reactions were performed in heptane, under dry nitrogen in conventional three-necked flasks, equipped with gas inlet, cooler, mercury check valve and magnetic stirring. The amounts of reagents are specified below. The yields of the products are calculated on the *reacted* carbonyl. Reaction times reported indicate the time required to bring the solution to reflux and the reflux time (e.g. 6 + 7 min indicates 6 min to reflux followed by 7 min reflux). After reaction the suspensions were filtered under N_2, reduced to small volume under vacuum and purified on t.l.c. plates (Kieselgel P.F.Merck, eluants mixtures of petroleum ether and diethyl ether in 9:1 v/v ratio).

2.1.3. Analysis of the organometallic complexes

The IR spectra (solvent heptane) were obtained on a Brucker Vector 22 (KBr cells, path length 0.5 mm). The ^1H, ^{13}C and the ^{29}Si NMR spectra were registered on a JEOL Eclipse 400. Solvents used were $CDCl_3$ and CD_3OD (for the complexes presumably containing *thp*). The EI and CI mass spectra were obtained on a Finnigan-Mat TSQ-700 mass spectrometer (Servizio di spettrometria di massa, Dipartimento di Scienza e Tecnologia del Farmaco, Università di Torino). The ESI (positive and negative ions) mass spectra were obtained on a Finnigan-Mat LCQ Duo spectrometer under the following conditions: steath gas (necessary for the nebulisation process) flow rate 80 (arb. units), aux. gas flow rate 0, spray voltage 4.50 kV, capillary temp. 270 K, capillary voltage 10 V, tube lens offset 0 V.

2.1.4. Characterization of the sol–gel materials

The chemical composition of the material obtained from SBA-15 (*Co/SBA-15*) was determined by inductively coupled plasma-mass spectrometry (ICP-MS) [ITECON s.r.l., Nizza Monferrato, AT, Italy] under the following conditions: alkaline fusion of the materials with $LiBO_3$ at 1100 °C for 30 min. Dissolution in ultrapure water contaning about 2% of HNO_3 followed by ICP-MS analysis.

The FT-IR spectra were obtained on a Bruker Equinox 55 (KBr cells, path length 0.5 mm) with pyroelectric DTGS detector (data elaboration through Opus 5.0 software) and ATI-Mattson (data elaboration software WinFIRST). The spectrum of *Co/SBA-15* was recorded under vacuum: the sample was pressed in the form of self-supporting wafers and placed into a IR cell equipped with KBr windows, permanently attached to a high vacuum line (residual pressure 1.0×10^{-6} Torr).

Thermogravimetric analyses were performed using a TA Instruments SDT 2960 apparatus. The analyses were performed under a N_2 stream (10–100 cm^3/min) using 10–15 mg samples and heating at 10 °C/min from 25 to 800 °C, operating system TA 2000 Operative System.

The XRD analyses were performed on a Thermo ARL X'TRA 48 instrument using the Cu Kα radiation (λ = 1.54062 Å). Scanning Electron Microscopy (SEM) analyses were performed using a LEO 1450 VP instrument. The surface of the solids was coated with a thin gold layer to ensure surface conductivity. Energy Dispersive X-ray spectroscopy (EDS) was used to provide rapid semiquantitative elemental analyses on the sample surface.

2.2. Reaction of $Co_2(CO)_8$ with pol, bud and mbo

2.2.1. Reaction with pol

Two grams (ca 7.0 mmol) of the cobalt carbonyl were suspended in heptane under N_2 and 3.0 cm^3 of the alkyne (ca 12 mmol) were added. After reflux (7 + 8 min) the colour turned deep-red. T.l.c. purification showed the presence of three bands, blue, brown and brown (trace amounts, not investigated) and of a red band (**1**) in 90% yields. Some decomposition was also observed.

*2.2.1.1. Complex (**1**).* Anal. Calc. (formula): C, 35.67; Co, 31.89; H, 2.16. Found: C, 35.5; Co, 31.9; H, 2.2%. IR (heptane): 2088 m, 2048 s, 2025 vs, 2016 s(sh), 2005 m(sh), 1974 w, cm^{-1}. ^1H NMR: 3.90 m (2H, CH_2), 3.07 m (2H, CH_2), 2.66 m (3H, CH_3), 2.17 d (1H, OH). Mass spectra (*m*/*z*): 370, M+; (mass numbers) [M−nCO]+ (*n* = 1–6).

2.2.2. Reaction with bud

The synthesis and molecular structure of complex (**2**) has been previously reported [11]. An improved synthetic method has been described [6].

2.2.3. Reaction with mbo

Two grams (ca 7.0 mmol) of the cobalt carbonyl were suspended in heptane and 1.5 cm^3 of the alkyne (ca 20 mmol) were added. After reflux (8 + 8 min) the colour turned dark red. T.l.c. showed the presence of only one orange-red band (**3**) in about 70% yields and some decomposition.

*2.2.3.1. Complex (**3**).* Anal. Calc. (formula): C, 35.67; H, 2.16; Co, 31.89. Found: C, 35.7; H, 2.2; Co, 32.0%. IR (heptane): 2096 m, 2055 vs, 2033 vs, 2025 s(sh), 2009 m(sh), cm^{-1}. ^1H NMR (CD_3OD): 6.31 s (1H, HC≡), 3.59, 3.29 s (1H, OH), 1.64 m (3H, CH_3), 1.54–1.06 m (3H, CH_3). ^{13}C NMR: 17.03 s (CH_3), 30.4–32.5 t (CH_3), 57.0 s (C(OH)), 71.8 s (C≡C), 145.2 t (HC≡), 200.0 s (vb) (CO). Mass spectra (*m*/*z*) = 370, M^+.

2.3. Synthesis of the phosphine-substituted complexes

2.3.1. Reaction of $Co_2(CO)_8$ with dpts

About 1.0 g [ca 3.5 mmol] of $Co_2(CO)_8$ was dissolved in heptane under N_2 and 1.0 cm^3 [ca 3.0 mmol] of *dpts* was added. The milky suspension was refluxed (7 + 7 min), after which time the colour turned to dark brown. T.l.c. showed the presence of a dark brown

band (40%, (**4**)), trace amounts of a blue complex (not collected) and a red band (50%, (**5**)).

*2.3.1.1. Complex (**4**).* Anal. Calc. (formula): C, 46.96; H, 4.20; Co, 17.10; P, 4.49; 4.40. Found: C, 47.0; H, 4.3; Co, 17.2; P, 4.40%.

M.w. 690. IR (heptane): 2082 m, 2039 vs, 2027 m(sh), 2006 w, 1850 m, 1831 m, cm^{-1}. ^1H NMR: 7.87–7.20 (broad), 6.70 s(b) [10 H, Ph), 4.04–3.49 d(b) (6H, CH_2, Et), 3.56 d (2H, CH_2), 2.35 s(vb) (2H, CH_2), 0.88 s (9H, CH_3). ^{13}C NMR: 18.39 s (CH_3), 30.92 s (CH_2), 128.51 s, 130.96 s (Ph), 206.98 d (CO). ^{31}P NMR: 34.9 s, 43.8 s. C.I. mass spectrum: 689 *m/z* (medium intensity), 664 (highly intense, -C_2H_2), 647 (intense). ESI mass spectrum: 733 *m/z* (M^+ + solvent (CH_3OH)), doubly charged ion at 345 *m/z*.

*2.3.1.2. Complex (**5**).* Anal. Calc. (formula): C, 53.18; H, 5.59; Co, 53.18; P, 5.97. Found: C, 53.2; H, 5.6; Co, 11.4; P, 6.0%. M.w. 1038.

IR (heptane): 1978 w, 1960 s, cm^{-1}. ^1H NMR: 7.70 s, 7.40 s (20 H, Ph), 4.20 s (12 H, CH_2, Et), 2.50 s (4H, CH_2), 1.20 s (18 H, CH_3), 0.80 s (4H, CH_2). ^{13}C NMR: 17.2 d (CH_3), 48.1 s (CH_2), 57.0 s (CH_2), 128.7–131.8 mm (Ph), 198.0 (vb) (CO). ^{31}P NMR: 59.6 s (weak), 67.1 s (very intense). C.I. mass spectrum: 1002 m/z (low intensity), 786 (intense), 740 (highly intense). ESI mass spectrum: decomposition.

*2.3.2. Reaction of $Co_2(CO)_6$(pol) (**1**) with dpts*

About 0.5 g [ca 1.4 mmol] of the cobalt complex were dissolved in heptane under N_2 and a small excess of *dpts* was added. The solution was brought to reflux (6 + 6 min). T.l.c. showed the presence of a red band (80%, (**6**)) and of some decomposition.[12]

*2.3.2.1. Complex (**6**).* Anal. Calc. (formula): C, 53.74; H, 5.68; Co, 10.47; P, 5.68. Found: C, 53.7; H, 5.7; Co, 10.5; P, 5.7%. M.w. 1094.

IR (heptane): 2056 m, 2013 vs, 1967 (C vs(sh), 1958 vs, 1933 m-w(sh), cm^{-1}. ^1H NMR: 7.80 s, 7.50 s, 7.27 s (20H, Ph), 3.70 d (8H, CH_2), 2.40 d(b) (4H, CH_2), 1.70 s (1 H, OH), 1.50 s(b) (12H, CH_2, Et), 1.10 d (18H, CH_3, Et), 1.00–0.20 m (b) (3H, Me). ^{13}C NMR (CD_3OD): 17.1 d, 22.2 s, 57.0 s, 58.4 s, 128.6–132.0 m (Ph), 200.0 (vb) (Co(CO)). ^{31}P NMR: 49.3 s, 39.0 s. C.I. mass spectrum: 1058 *m/z*. ESI mass spectrum: decomposition.

2.3.3. Reaction of $Co_2(CO)_6$(mbo) with dpts

About 1.0 g (ca 2.5 mmol) of (**3**) were dissolved in heptane–toluene (50:50 vv: the complex is sparingly soluble in heptane) and 1.0 cm^3 of *dpts* were added. After reflux (8 + 8 min), t.l.c. of the dark red solution showed the presence of only one dark red band (**7**) in about 90% yields.

*2.3.3.1. Complex (**7**).* Anal. Calc. (formula): C, 54.05; H, 5.94; Co, 10.67; P, 5.68. Found: C, 54.1; H, 5.9; Co, 10.7; P, 5.6%. M.w. 1110

IR (heptane): 2060 w, 2021 vs, 1967 vs, 1941 w, 1765 m, 1712 m, cm^{-1}. ^1H NMR (very broad signals): 7.43 s, 3.76 s, 2.31 s, 1.18 s. ^{13}C NMR (CD_3OD): 1.29 s, 18.33 s, 23.0 d, 33.84 s, 58.65 s (C≡C), 127.52–132.19 m, 196.0 (vb) (CO). ^{31}P NMR: 35.3 s. C.I. mass spectrum: 1074. ESI mass spectrum: 555 (M^{++}).

2.3.4. Reaction of $Co_2(CO)_6$(bud) with dpts

About 1.0 g [2.8 mmol ca] of the cobalt complex (**2**) and 1.0 cm^3 [2.6 mmol ca] of *dpts* were dissolved in heptane under N_2: a milky suspension was obtained. This was refluxed (7 + 7 min). T.l.c. purification showed the presence of a dark brown band (40%, (**8**)), a blue band (tr., not investigated) and a red band (50%, *parent complex).*

A"direct" synthetic pathway is the following. Reaction of $Co_2(CO)_8$ with *bud* as previously described [6]. After reflux (8 + 10 min) the solution is cooled, a slight excess of *dpts* is added and the suspension refluxed again (4 + 8 min). T.l.c. yields (**8**) in about 30% yields.

*2.3.4.1. Complex (**8**).* Anal. Calc. (formula): C, 53.38; H, 5.69; Co, 10.50; P, 5.52. Found: C, 53.4; H, 5.7; Co, 10.6; P, 5.50%. M.w. 1124.

IR (heptane): 2090 m, 2047 vs, 2018 vs, 1974 s, 1965 s(sh), cm^{-1}. ^1H NMR: (broad signals): 7.35 s (Ph), 3.70 s (CH_2Et), 2.30 s (CH_2), 1.62 s (CH_2 bud), 1.14 s (CH_3), 0.53 s (OH). ^{13}C NMR: 3.86 s, 18.25 s, 25.53 s, 58.59 s, 62.51 s (CH_2OH), 85.98 s (C≡C), 128.51–132.31 m, 136.11 t, 206.94 s (CO). ^{31}P NMR: 35.2 s, 50.1 s. C.I. mass spectrum: 1088. ESI mass spectrum: 562 (M^{++}).

2.4. Other reactions

*2.4.1. Reaction of $Co_2(CO)_6$(pol) (**1**) with tsi*

0.75 g (ca 2.0 mmol) of (**1**) were reacted with 2 cm^3 (ca 8 mmol) of *tsi* in heptane, under Ar for 5 min (up to reflux) and 10 min reflux. The t.l.c. plates showed the presence of a dark red band ((**9**), ca 50%) and of decomposition (blue, 40%).

*2.4.1.1. Complex (**9**).* $Co_2(CO)_6[H_3CC{\equiv}CCH_2CH_2OC(=O)NH(CH_2)_3$-$Si(OEt)_3]$: Anal. Calc. (formula): C, 40.91; H, 4.38; Co, 29.22; Si, 4.54. Found: C, 41.0; H, 4.4; Co, 29.3; Si, 4.4%.

IR (heptane): 2090 m-s, 2050 vs, 2028 vs, 2019 s(sh), 2006 m(sh), 1725 s, 1699 m(b) cm^{-1}. ^1H NMR: 4.36 b (1H, NH), 3.80 d (2H, NCH_2), 3.21 b (4H, ≡CCH_2CH_2), 2.64 s (4H, $(CH_2)_2$), 1.64 b (6H, SiCH_2), 1.20 s (9H, CH_3), 0.62 s(b) (CH_3C≡). ^{13}C NMR: 7.80 m, 18.34 s, 20.2–23.3 m, 32.3 s, 43.3 d, 45.5 m, 58.5 d, 66.3 s (CH_3, CH_2), 92.0 s, 93.8 s (C≡C), 149.0 s (C(=O)O), 154.1 s, 156.2 d, 199.6 b (CO). ^{29}Si NMR: −42.22 vs. EI-MS: *m/z* 616 weak, release of 6 CO and competitive complex fragmentation.

2.5. Synthesis of the hybrid inorganic–organometallic materials

*2.5.1. Reaction of $Co_2(CO)_6$(pol) (**1**) with teos*

A saturated heptane solution of (**1**) (10 cm^3) was added to a saturated solution of ethanol (10 cm^3) containing 5 cm^3 of *teos*: the resulting solution was stirred and then evaporated under reduced pressure. The solid obtained was dried under air (sample *sga*). Another attempt consisted in mixing the saturated heptane solution of the complex with a saturated ethanolic solution of *teos* containing also 5 cm^3 of H_2O in which about 0.5 g of NaF had been dissolved. Gelation occurred more rapidly. The solution was stirred and evaporated under reduced pressure, then dried in air. The same material (*sga*) was obtained.

2.5.2. Reactions of $Co_2(CO)_6(dpts)_2$ with SBA-15

SBA-15 was treated under vacuum at 200 °C for 4 h in order to remove the water and activate the surface. After cooling, a solution of 50 mg of (**5**) in toluene was added. The suspension was then warmed at 60 °C and stirred for 24 h. The final product was filtered, washed several times with petroleum ether in order to dissolve eventual soluble cobalt complexes and dried at room temperature for 24 h.

2.6. Crystallography

Crystal and refinement data of (**1**), (**5**) and (**8**) are collected in Table 1.

*2.6.1. Complex (**1**)*

Crystals were obtained from a n-heptane solution. The reflection data have been collected on a Siemens P4 diffractometer equipped with a Bruker APEX CCD detector. The intensities have been corrected semi-empirically for absorption, based on symmetry equivalent reflections. The refinement was made using

Table 1
Crystal data and structure refinement details.[a]

Complex	$Co_2(CO)_6[\mu\text{-}\eta^2\text{-}(H_3CC{\equiv}CCH_2CH_2OH)]$ (**1**)	$Co_2(CO)_6[Ph_2PCH_2CH_2Si(OCH_2CH_3)_3]_2$ (**5**)	$Co_2(CO)_4[\mu\text{-}\eta^2\text{-}(C{\equiv}C(CH_2OH)_2)][Ph_2PCH_2CH_2Si(OCH_2CH_3)_3]_2$ (**8**)
Formula	$C_{11}\mathbf{H_8}Co_2O_7$	$C_{46}\mathbf{H_{70}}Co_2O_{12}P_2Si_2$	$C_{48}\mathbf{H_{62}}Co_2O_{12}P_2Si_2$
M	370.04	1051.00	1067.00
Crystal system	Monoclinic	Orthorhombic	Monoclinic
Space group	$P2_1/n$	$Pbca$	$P2_1/n$
a (Å)	19.3349(18)	14.3776(3)	15.396(3)
b (Å)	7.1829(6)	17.1866(4)	14.657(3)
c (Å)	20.7491(19)	22.2259(7)	25.467(3)
α (°)	90.	90.	90.
β (°)	84.031(2)	90.	90.
γ (°)	90.	90.	90.
U (Å^3)	2831.0(4)	5492.1(2)	5478.1(17)
Z	8	4	4
Crystal colour	Light yellow	Red	Red
Crystal dimensions (mm)	0.06 × 0.10 × 0.28	0.04 × 0.16 × 0.24	0.03 × 0.09 × 0.13
μ(Mo Kα) (mm^{-1})	2.368	0.76	0.76
Temperature (K)	120	293	293
θ Range	1.32–25.00	3.00–32.79	2.88–29.43
Total no. reflections	26882	67815	60339
Unique reflections	4981	9601	13658
R_{int}	0.037	0.10	0.15
No. of parameters	364	241	327
R_1[b] [$I_0 > 2\sigma(I_0)$]	0.0436[4385 obs.]	0.065[1944 obs.]	0.0724[2496 obs.]
R_1 (all data)	0.123	0.325	0.359
wR_2[b][$I_0 > 2\sigma(I_0)$]		0.165	0.165
wR_2 (all data)		0.200	0.213
Goodness-of-fit[c]	1.054	0.79	0.76

[a] Common items: wavelength (Mo Kα) = 0.71073 Å.
[b] $R_1 = \Sigma||F_o|-|F_c||/\Sigma|F_o|$, $wR_2 = [\Sigma(wFo^2-Fc^2)2/\Sigma w(F_o^2)^2]^{1/2}$.
[c] *G.O.F.* (**G**oodness **O**f **F**itness) = $\Sigma(wF_o^2-Fc^2)^2/$(no.of unique reflections − no. of parameters).

full-matrix least-squares on F^2. The asymmetric unit contains two molecules. All non-hydrogen atoms were refined anisotropically. The hydrogen atoms have been located and then kept fixed with U_{iso} set at 1.2 times U_{eq} of the corresponding C atom and 1.5 U_{eq} of the corresponding O atom.

Programs used were SHELXTL [13] for structure solution, refinement and molecular graphics, BRUKER AXS SMART (diffractometer control), SAINT (integration), SADABS (absorption correction)] [14]. The CIF file is deposited at CSD as CCDC 714073.

2.6.2. Complex (**5**)

The reflection data, using a crystal obtained from a heptane solution, have been collected on a Gemini R Ultra diffractometer [15]. The refinement was made using full-matrix least-squares on F^2. The hydrogen atoms, with the exclusion of those linked to the ethoxy groups, have been calculated and then kept riding with U_{iso} set at 1.2 times U_{eq} of the corresponding C atom. All other atoms have been refined anisotropically with the exclusion of atoms of ethoxy groups, that have been refined isotropically with restraints. This refinement strategy has been considered suitable owing to the very high thermal motion of the atoms.

Programs used were CRYSALISPRO [15] for data collection and correction and SHELXTL [13] for structure solution, refinement and molecular graphics. The CIF file is deposited at CSD as CCDC 738898.

2.6.3. Complex (**8**)

The reflection data, using a crystal obtained from a heptane solution, have been collected on a Gemini R Ultra diffractometer [15]. The refinement was made using full-matrix least-squares on F^2. The hydrogen atoms, with the exclusion of those of the OH groups and those linked to the ethoxy groups, have been calculated and then kept riding with U_{iso} set at 1.2 times U_{eq} of the corresponding C atom. All other atoms have been refined anisotropically with the exclusion of atoms of the ethoxy groups, that have been refined isotropically with restraints. The phenyl groups were also refined with the constrained exact hexagonal geometry. This refinement strategy has been considered suitable owing to the very high thermal motion of the atoms and to the poor quality of all crystals measured.

Programs used were CRYSALISPRO [15] for data collection and correction and SHELXTL [13] for structure solution, refinement and molecular graphics. The CIF file is deposited at CSD as CCDC 738899.

3. Results and discussion

The reactions performed during this work and leading to phosphine-substituted complexes and to inorganic–organometallic materials are summarized in Scheme 1.

3.1. Synthesis of the complexes $Co_2(CO)_6$(*pol*) and $Co_2(CO)_6$(*mbo*)

The reaction of $Co_2(CO)_8$ with *pol* gives high yields of the expected complex $Co_2(CO)_6(H_3CC{\equiv}CCH_2CH_2OH)$ (**1**) which shows the well known "pseudo-tetrahedral" structure first reported for $Co_2(CO)_6(PhC{\equiv}CPh)$ [16,17].

The reaction of $Co_2(CO)_8$ with *bud* and the structure of the resulting (**2**) have already been reported [11,6]. The reaction of the cobalt carbonyl with *mbo* gives $Co_2(CO)_6(HC{\equiv}C(CH_3)_2OH)$, (**3**) in high yields. Elemental analyses and spectroscopic evidence indicate that (**3**) contains an intact ligand and that no dehydration has occurred during the synthesis.

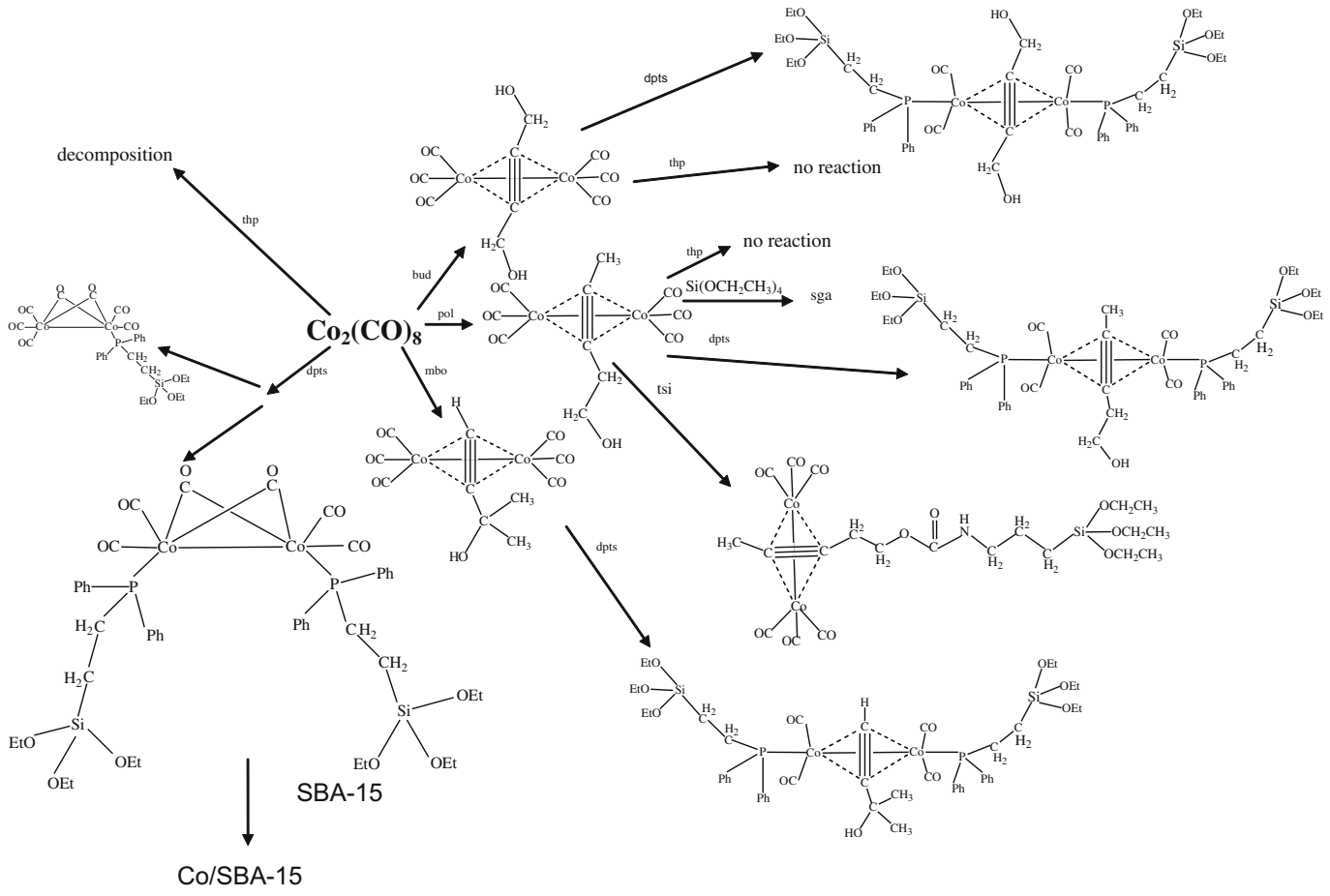

Scheme 1.

3.2. The reactivity of $Co_2(CO)_6$(pol)

By exploiting the reactivity of the cobalt-coordinated *pol* it was possible to build a new coordinated ligand [7]. Indeed (**1**) reacts with *tsi* to give good yields of the new complex $Co_2(CO)_6[H_3CC{\equiv}CCH_2CH_2OC(=O)NH(CH_2)_3Si(OEt)_3]$ (**9**) which has been characterized by spectroscopic analyses. Previous experience [6] indicates that this type of complexes can be easily grafted on *teos* and/or undergo oligomerization; this is presumably the reason why we could not obtain crystals suitable for a X-ray analysis.

For (**9**) the well known structure with C≡C perpendicular to the Co–Co bond can be proposed, with formula $Co_2(CO)_6[[\mu\text{-}\eta^2\text{-}(CH_3C{\equiv}C(CH_2CH_2)_2\ OC(=O)NH(CH_2)_2Si(OEt)_3]$.

3.3. The molecular structure of $Co_2(CO)_6[\mu\text{-}\eta^2\text{-}(H_3CC{\equiv}CCH_2CH_2OH)]$ (**1**)

The structure of (**1**) is shown in the Fig. 1 and relevant distances and angles are listed in Table 2 for both molecules.

The complex (Fig. 1 and Table 2) contains a pseudo-tetrahedral arrangement of two cobalt atoms and two carbon atoms of the elongated C≡C bond of the alkyne (Co(1)–Co(2) 2.4690(9) Å av., C(2)–C(3) 1.326(6) Å av.). Three terminal carbonyl groups are bound to each cobalt atom. The elongated triple bond is perpendicular to the Co–Co bond according to a well known geometry (Co···C(alkyne) 1.972(4) Å av.). The X-ray analysis shows that no loss of the alkyne functionality has occurred.

The C(2)–C(3) distance is well comparable with those in $Co_2(CO)_6(C_2R_2)$ with R = Ph, CO_2Me,Bu^t, lying in the range 1.33(3)–1.36(1) Å [16]. In the latter compounds the Co–Co and the Co···C(alkyne) distances are in the ranges 2.460(1)–2.477(3) and 1.92(2)–1.987(2) Å, respectively.

3.4. Reactions of $Co_2(CO)_8$ and of (**1**),(**2**), (**3**) with the phosphinic ligands

3.4.1. Reactions of $Co_2(CO)_8$ with dpts

The reaction of the cobalt carbonyl with *dpts* yields two products, (**4**) and (**5**). In spite of many attempts (by changing solvent and conditions) crystals of (**4**) suitable for X-ray analysis could not be obtained. The IR spectra indicate the presence of two bridging carbonyls and the NMR data and the CI and ESI mass spectra exclude the possibility that (**4**) is a $Co_4(CO)_8(\mu\text{-}CO)_2(L)$ butterfly [18] or a $Co_3(CO)_7(\mu\text{-}CO)_2(\mu_3\text{-}L)$ methylidyne complex [19]. The proposed structure is therefore $Co_2(\mu\text{-}CO)_2(CO)_5$(dpts) and is shown in the Fig. 2 (below): it is known that the parent compound $Co_2(CO)_8$ in the solid-state has a structure with two bridging carbonyls [20]. To our knowledge in the literature a phosphine-monosubstituted dicobalt complex has been reported with only terminal CO groups [21] and a trisubstituted complex with formula $Co_2(\mu\text{-}CO)_2(CO)_3[P(CH_3)_2Ph]_3$ [22] is known.

In contrast, the reaction of the cobalt carbonyl with *thp* resulted only in decomposition. No soluble products could be isolated.

3.4.2. Reactions of $Co_2(CO)_6$(pol) with dpts

Complex (**1**), whose structure is described above, has been reacted with *dpts*. Very high yields (90%) of the unique (**6**) could be obtained. Unfortunately no crystals suitable for X-ray analyses

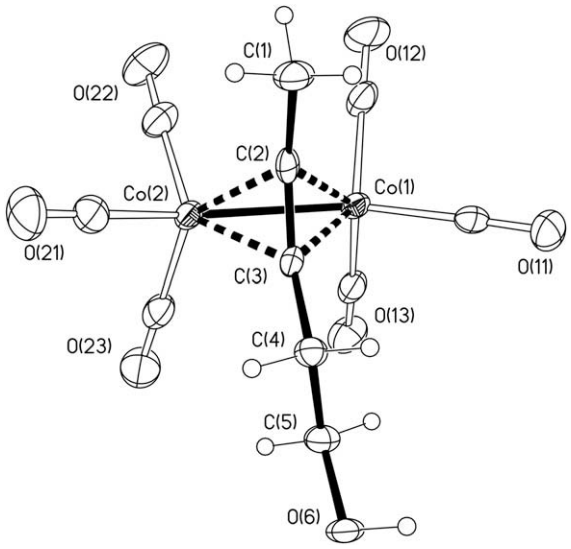

Fig. 1. ORTEP plot (50%) of one molecule of $Co_2(CO)_6[\mu\text{-}\eta^2\text{-}(H_3CC{\equiv}CCH_2CH_2OH)]$ complex with atom labelling.

Table 2
Relevant bond lengths (Å) and angles (°) for the two independent molecules.

Co(1)–Co(2)	2.4722(9)	2.4658(8)
Co(1)–C(11)	1.784(5)	1.796(5)
Co(1)–C(12)	1.823(5)	1.835(5)
Co(1)–C(13)	1.817(5)	1.824(5)
Co(1)–C(2)	1.969(4)	1.955(4)
Co(1)–C(3)	1.974(4)	1.974(4)
Co(2)–C(21)	1.790(5)	1.779(5)
Co(2)–C(22)	1.825(5)	1.811(5)
Co(2)–C(23)	1.815(5)	1.828(5)
Co(2)–C(2)	1.969(4)	1.983(4)
Co(2)–C(3)	1.966(4)	1.963(4)
C(1)–C(2)	1.489(6)	1.494(6)
C(2)–C(3)	1.334(6)	1.319(6)
C(3)–C(4)	1.484(6)	1.501(6)
C(4)–C(5)	1.514(6)	1.529(6)
C(5)–O(6)	1.430(5)	1.419(6)
C(3)–C(2)–C(1)	143.9(4)	144.8(4)
C(2)–C(3)–C(4)	142.0(4)	143.2(4)
C(3)–C(4)–C(5)	113.1(4)	111.6(4)
O(6)–C(5)–C(4)	113.0(4)	112.2(4)

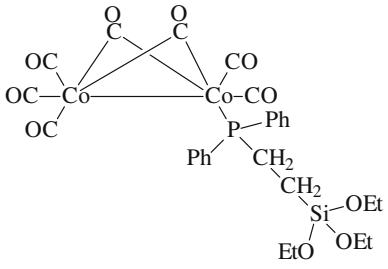

Fig. 2. Proposed structure of (**4**), $Co_2(CO)_7$(dpts).

could be obtained. Spectroscopic results indicate that this could be the disubstituted $Co_2(CO)_4$(pol)$(dpts)_2$. The proposed structure is analogous to that of (**8**).

3.4.3. Reaction of complex $Co_2(CO)_6$(mbo) with dpts

Complex (**3**) reacts with *dpts* giving, as the unique product, (**7**) in good yields. Spectroscopic evidence indicates that this complex, also, is a disubstituted product. The proposed structure is analogous to that of (**8**).

3.4.4. Reactions of $Co_2(CO)_6$(bud) with dpts

The cobalt complex (**2**) whose structure had already been reported [11], has been reacted with *dpts*: one complex only, (**8**), was obtained in high yields.

3.4.5. Reactions of $Co_2(CO)_6$(pol) and of $Co_2(CO)_6$(bud) with thp

As already shown for $Co_2(CO)_8$, also from these reactions no phosphine-substituted complexes could be obtained. Only some decomposition products were found. This is probably due to the low electron donor power of the phosphine (low σ Taft). Therefore *thp* is not suitable for grafting cobalt carbonyls on inorganic substrates.

3.5. The molecular structures of the phosphine-substituted complexes

3.5.1. The molecular structure of $Co_2(CO)_6(dpts)_2$

The structure of the complex is shown in Fig. 3 and relevant distances and angles are in Table 3. The molecule lies on a crystallographic inversion centre, therefore all substituents on Co atoms are in a staggered or *anti* configuration.

The comparison with the parent compound $Co_2(\mu\text{-}CO)_2(CO)_6$ [20] shows that the double substitution results in the "loss" of the bridging carbonyls and in the elongation of the Co–Co bond distance (2.661(1) Å *versus* 2.526(1) Å). A number of disubstituted complexes with phosphinic terminal ligands shows the range of the Co–Co bond distances around 2.66 Å. Selected examples are the $Co_2(CO)_6L_2$ derivatives where L = PPh_3 [23], $P(OPh)_3$ [24], $P(CH_3)_3$ [25], $PPh_2(CH_2P(=O)Ph_2)_3$ [26a,b], $PPh_2(C_6H_4N(CH_3)_2)$ [27], $P(CH_3)_2Ph$ [22], $PPh_2(CH_2C(=O)Ph)$ [28], $P(OPr^i)_3$ [29].

3.5.2. The molecular structure of $Co_2(CO)_4$(bud)$(dpts)_2$ (**8**)

It belongs to the well known carbonyl complexes bearing an acetylenic moiety perpendicularly π-bonded to a Co–Co bond and six terminal ligands. Every Co atom links two CO groups and a phosphine ligand. The structure of (**8**) is shown in Fig. 4 and relevant distances and angles are in Table 3.

The four terminal CO ligands are eclipsed and the Co–Co bond distance (2.472 Å) well compares with other similar complexes

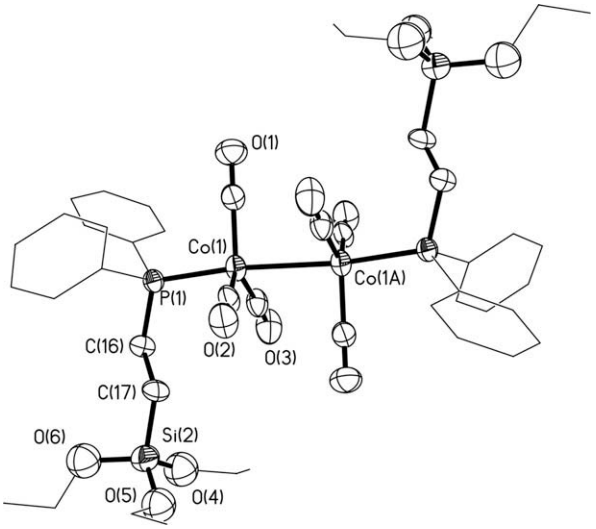

Fig. 3. ORTEP view (30% probability) of (**5**) $Co_2(CO)_6[Ph_2PCH_2CH_2Si(OCH_2CH_3)_3]_2$, with atom labelling. Atoms with label A are related by the crystallographic inversion centre.

Table 3
Relevant bond lengths (Å) and angles (°) for (**5**) and (**8**).

(5)	Co(1)–Co(1A)	2.6611(11)
	Co(1)–C(1)	1.774(7)
	Co(1)–C(2)	1.779(6)
	Co(1)–C(3)	1.738(7)
	Co(1)–P(1)	2.1904(12)
	P(1)–C(16)	1.819(5)
	C(16)–C(17)	1.527(6)
	C(17)–Si(2)	1.852(5)
	C(3)–Co(1)–C(2)	120.8(3)
	C(3)–Co(1)–C(1)	121.3(3)
	C(2)–Co(1)–C(1)	116.4(2)
	C(3)–Co(1)–Co(1A)	80.84(15)
	C(2)–Co(1)–Co(1A)	87.47(15)
	C(1)–Co(1)–Co(1A)	89.78(16)
	P(1)–Co(1)–Co(1A)	172.31(6)
(8)	Co(1)–Co(2)	2.4725(14)
	Co(1)–C(11)	1.762(9)
	Co(1)–C(12)	1.772(11)
	Co(1)–C(3)	1.960(7)
	Co(1)–C(2)	1.970(8)
	Co(1)–P(1)	2.207(2)
	Co(2)–C(21)	1.789(9)
	Co(2)–C(22)	1.798(10)
	Co(2)–C(3)	1.942(7)
	Co(2)–C(2)	1.983(8)
	Co(2)–P(2)	2.219(2)
	C(1)–O(1)	1.391(9)
	C(1)–C(2)	1.497(10)
	C(2)–C(3)	1.312(9)
	C(3)–C(4)	1.543(10)
	C(4)–O(2)	1.407(9)
	P(2)–Co(2)–Co(1)	153.86(8)
	P(1)–Co(1)–Co(2)	151.86(8)
	O(1)–C(1)–C(2)	110.2(7)
	C(3)–C(2)–C(1)	140.9(7)
	C(2)–C(3)–C(4)	137.3(8)
	O(2)–C(4)–C(3)	108.2(7)

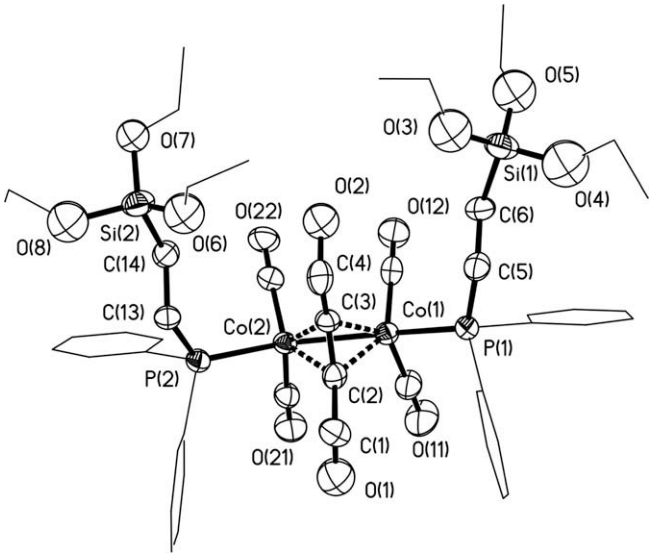

Fig. 4. ORTEP plot (30% probability) of (**8**), $Co_2(CO)_4[\mu\text{-}\eta^2\text{-}(C{\equiv}C(CH_2OH)_2)][Ph_2PCH_2CH_2Si(OCH_2CH_3)_3]_2$, with atom labelling.

(see (**1**)). The two phosphinic ligands are *cis* with respect to the Co–Co bond. The 1,4-butyn-diol, $HOCH_2C{\equiv}CCH_2OH$, with the elongation of the C≡C bond, assumes the structure of an alkene with the CH_2OH substituents related by a non crystallographic mirror plane defined by the Co(1)Co(2) atoms and by the middle point of the C(2)–C(3) bond (Fig. 5).

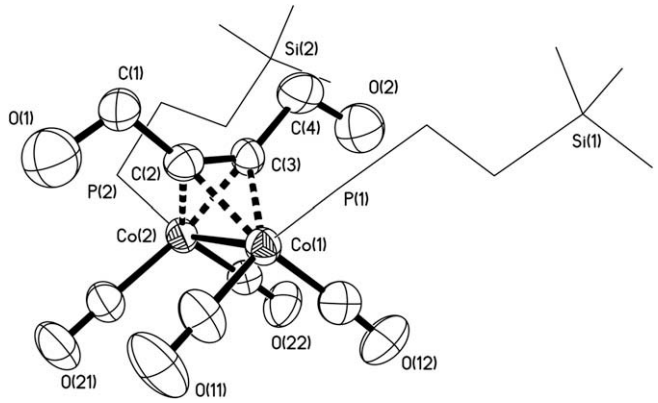

Fig. 5. ORTEP plot (30% probability) showing the geometry of the alkyne ligand and the eclipsed configuration of the CO groups in (**8**).

3.6. The synthesis and characterization of hybrid materials

3.6.1. Reaction of (*1*) with tsi

The reactivity of (**1**) can be exploited for grafting directly the complex to *teos*. We could obtain, indeed, a new inorganic–organometallic material (*sga*) which has been characterized by spectroscopic techniques. The material *sga* is a very fine amorphous powder (as shown by a XRD analysis) with a relatively low surface area of 150 m^2/g and a very irregular distribution of the pore dimensions. Unfortunately the Raman spectrum showed the fluorescence typical of the presence of metal centres. The IR (KBr pellets) showed the following signals: 3500–3100 vb, 2900 b (ligand CH_3, CH_2, surface OH), 2095, 2054, 2027 (ν_{CO}), 1710 (O–C), 1553 (O–Si), 1250–900 (skeletal vibration of SiO_2) [30]. The TGA analysis showed losses of weight between 50 and 100 °C (loss of residual solvent) and at 280 °C (loss of CO and organic fragments).

3.6.2. Reactions of (*5*) with SBA-15

Due to the presence of two triethoxy groups, (**5**) was successfully anchored on the surface silanols of SBA-15 mesoporous support. The chemical analysis performed by ICP-MS showed that the final hybrid material based on SBA-15 (*Co/SBA-15*), contains 22.7 and 0.6 mg/g of Co and P, respectively.

Particular attention was devoted to the investigation of the morphological and structural properties of the mesoporous silica after reaction with (**5**). The morphology of the pristine SBA-15, detected by scanning electron microscopy, was not modified upon anchoring. *Co/SBA-15* preserved, in fact, a rod-like morphology with particle dimensions around 1 μm, typical of the pristine support (Fig. 6). In addition, EDS analysis highlighted an homogeneous distribution of cobalt in the final material according to the ICP-MS analysis.[31]

X-ray diffraction pattern of pristine SBA-15 (Fig. 6B, curve a) shows three distinct reflections: one intense peak at 0.87° 2θ and two weak reflections at 1.5 and 1.7 2θ, which can be indexed as the (1 0 0), (1 1 0) and (2 0 0) planes related to the hexagonal pore arrray of SBA-15.[10] This pattern was also preserved after anchoring. However, *Co/SBA-15* showed a decrease of the peak intensities, along with a shift to higher 2θ, which is assigned to the immobilization of cobalt cluster inside the SBA-15 pores (Fig. 6B, curve b).

Particular attention was also devoted to the investigation of the vibrational profiles of the porous material before and after reaction with the cobalt complex. The Infrared spectrum of *Co/SBA-15* recorded under vacuum conditions, was compared with that of the pristine support (Fig. 7). The spectrum of SBA-15 (Fig. 7, solid lines) in the range 4000–3000 cm^{-1} showed two different signals. The peak at 3745 cm^{-1} is due to the stretching of isolated silanol

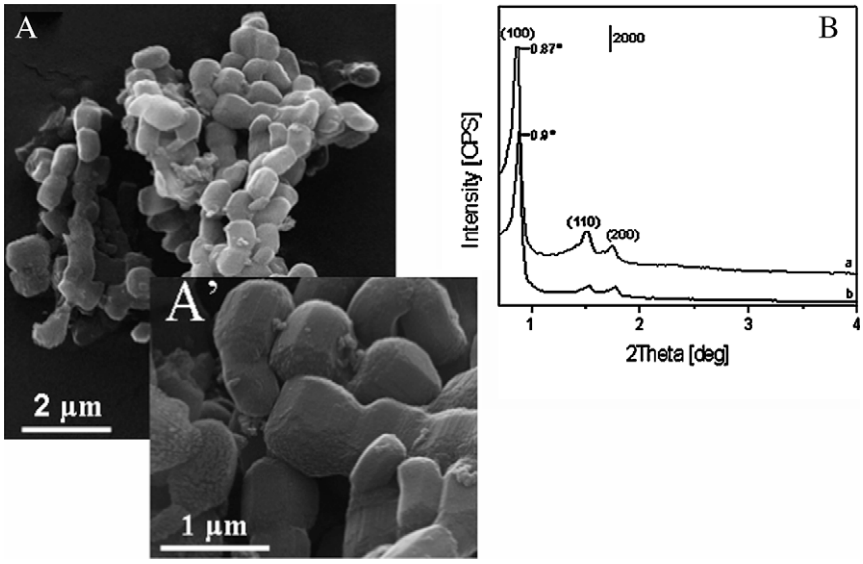

Fig. 6. SEM micrograph at lower (A) and higher magnification (A′) of Co/SBA-15. X-ray profiles of SBA-15 (a) and Co/SBA-15 (b) are reported in B.

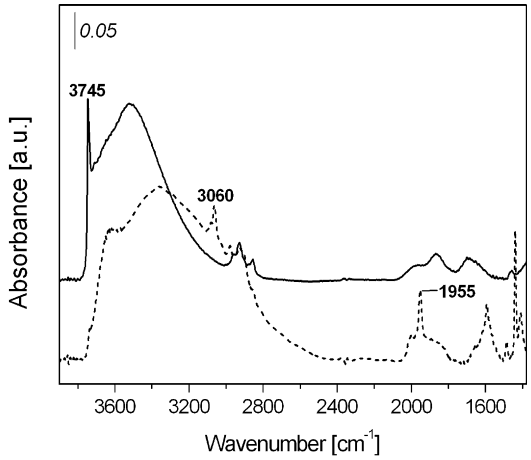

Fig. 7. IR spectra under vacuum conditions of SBA-15 (solid line) and Co/SBA-15 (short dashed line).

groups (Si–OH). The broad band in the 3700–3200 cm^{-1} range is assigned to Si–OH involved in hydrogen bonds. After reaction with (**5**), (Fig. 7, short dashed lines), the intensity of the isolated silanols drastically decreased and the shape of the broad band al lower wavenumber (around 3500 cm^{-1}) was modified.

These results suggested that a significant fraction of silanols of SBA-15 were involved during the grafting reaction with (**5**).

In addition, the typical absorptions of (**5**) (bands at 3060 and 1955 cm^{-1}, assigned to the ν(C–H) of phenyl groups and ν(CO), respectively) were found in the vibrational profile of *Co/SBA-15*, confirming that the complex structure was preserved during the anchoring procedure.

4. Conclusions

The results obtained indicate that starting from $Co_2(CO)_8$ and alkynols it is possible to obtain substituted complexes of formula $Co_2(CO)_6L$ where the ligand L still maintains intact the OH functionalities. The reactivity of these functionalities can be exploited to form hybrid inorganic–organometallic materials, as shown by the synthesis of (**9**) and by the "direct" grafting of (**1**) on *teos*.

Starting from cobalt centres with coordinated alkynols it is possible to obtain new functionalized complexes: these are mono- and disubstituted phosphine complexes with structures predictable on the basis of literature reports (even if, in some instances, the disposition of the ligands were not predictable with certainty). The derivatives containing *dpts* are suitable for grafting to sol–gel silica containing materials using the triethoxysilyl functionalities. This behaviour had already been observed for ruthenium carbonyl clusters [9]. In the case of cobalt, however, after grafting the unmodified cluster was found.

The above results show that the synthetic approach followed in this work may lead to a wide variety of inorganic–organometallic materials useful for catalysis and other applications.

References

[1] (a) R.J.P. Corriu, D. Leclerq, Angew. Chem., Int. Ed. 35 (1996) 1420–1436;
(b) U. Schubert, J. Chem. Soc., Dalton Trans. (1996) 3343–3348.
[2] (a) A. Choualeb, J. Rosé, P. Braunstein, R. Welter, Organometallics 22 (2003) 2688–2693;
(b) A. Choualeb, P. Braunstein, J. Rosé, S.E. Bouaud, R. Welter, Organometallics 22 (2003) 4405–4417;
(c) A. Choualeb, P. Braunstein, J. Rosé, R. Welter, Inorg. Chem. 43 (2004) 57–71.
[3] G. Gervasio, D. Marabello, E. Sappa, A. Secco, J. Organomet. Chem. 690 (2005) 3730–3736.
[4] (a) G. Gervasio, D. Marabello, E. Sappa, A. Secco, J. Organomet. Chem. 690 (2005) 3755–3764;
(b) G. Gervasio, D. Marabello, E. Sappa, A. Secco, Can. J. Chem. 84 (2006) 337–344.
[5] (a) G. Gervasio, D. Marabello, P.J. King, E. Sappa, A. Secco, J. Organomet. Chem. 671 (2003) 137–144;
(b) G. Gervasio, D. Marabello, P.J. King, E. Sappa, A. Secco, J. Organomet. Chem. 689 (2004) 35–42;
(c) G. Gervasio, D. Marabello, E. Sappa, A. Secco, J. Organomet. Chem. 690 (2005) 1594–1599.
[6] A. Arrais, E. Boccaleri, E. Sappa, A. Secco, J. Sol–Gel Sci. Technol. 38 (2006) 283–292.
[7] A. Arrais, E. Sappa, A. Secco, J. Cluster Sci. 18 (2007) 535–548.
[8] G. Gervasio, D. Marabello, E. Sappa, A. Secco, J. Cluster Sci. 18 (2007) 67–85.
[9] F. Carniato, A. Secco, G. Gatti, L. Marchese, E. Sappa, J. Sol–Gel. Sci. Technol. (2009), doi:10.1007/s10971-009-2018-y.
[10] D. Zhao, J. Feng, N. Melosh, G.H. Fredrickson, B.F. Chmelka, G.D. Stucky, Science 279 (1988) 548–552.
[11] M. Gruselle, B. Malezieux, J. Vaissermann, H. Amouri, Organometallics 17 (1998) 2337–2343.
[12] For comparison, the NMR data for *dpts* are: ^{13}C. 6.32 d, 18.43 s, 20,75 d, 58.56 s, 128.5 d, 132.9 d, 138.9 d. ^{31}P NMR: −8.5. ^{29}Si NMR: −46.0 d.
[13] M. Sheldrick, SHELXTL, Version 5.1, Bruker AXS inc., Madison, 1997.
[14] SMART, SAINT, SADABS, XPREP Software for CCD Diffractometers, Bruker AXS inc., Madison, WI.

[15] Oxford Diffraction Ltd., Abingdon, UK.
[16] D. Gregson, J.A.K. Howard, Acta Crystallgr. Sect. C (1983) 39 1024.
[17] R. Bianchi, G. Gervasio, D. Marabello, An electron density study, in: XXXI Congresso Nazionale Associazione Cristallografica Italiana, Parma, Italy, 18–21 September 2001.
[18] E. Sappa, A. Tiripicchio, A.J. Carty, G.E. Toogood, Prog. Inorg. Chem. 326 (1987) 437.
[19] D. Seyferth (Ed.), Adv. Organomet. Chem., vol. 14, Academic Press, N.Y., 1976, pp. 97–144.
[20] P.C. Leung, P. Coppens, Acta Crystallogr. Sect. B 39 (1983) 535.
[21] D.Z. Wang, B.F. Wu, Q.T. Hu, Acta Sci. Nat. NeMongol 24 (2003) 284.
[22] S.A. Liewellyn, M.L.H. Green, A.R. Cowley, Inorg. Chim. Acta 359 (2006) 3785–3789.
[23] N. Casati, P. Macchi, A. Sironi, Angew. Chem., Int. Ed. 44 (2005) 7736–7739.
[24] M. Haumann, R. Meijboom, J.R. Moss, A. Roodt, J. Chem. Soc., Dalton Trans. (2004) 1679–1786.
[25] R.A. Jones, M.H. Seeberger, A.L. Stuart, B.R. Whittlesey, T.C. Wright, Acta Crystallogr., Sect. C 42 (1986) 399.
[26] (a) R. Weber, U. Englert, B. Ganter, W. Keim, M. Mothrath, J. Chem. Soc., Chem. Commun. (2000) 1419;
(b) V.B. Golovko, L.J. Hope-Weeks, M.J. Mays, M. McPartlin, A.M. Sloan, A.D. Woods, New J. Chem. 28 (2004) 527–534.
[27] L. Brammer, J.C.M. Rivas, C.D. Spilling, J. Organomet. Chem. 609 (2000) 36–43.
[28] P. Braunstein, D.G. Kelly, Y. Dusausoy, D. Bayeul, M. Lanfranchi, A. Tiripicchio, Inorg. Chem. 33 (1994) 233–242.
[29] D.H. Farrar, A.J. Lough, A.J. Poe, T.A. Stromnova, Acta Crystallogr., Sect. C 51 (1995) 2008.
[30] For comparison the IR spectrum (KBr pellets) of the ligand pol is: 3400–3100 vb, 2970–2750 b, 1400, 1050 (vs) cm^{-1}.
[31] C.-L. Lin, Y.-S. Pang, M.-C. Chao, B.-C. Chen, H.-P. Lin, C.-Y. Tang, C.-Y. Lin, J. Phys. Chem. Solids 69 (2008) 415–419.